General Disclaimer

One or more of the Following Statements may affect this Document

- This document has been reproduced from the best copy furnished by the organizational source. It is being released in the interest of making available as much information as possible.

- This document may contain data, which exceeds the sheet parameters. It was furnished in this condition by the organizational source and is the best copy available.

- This document may contain tone-on-tone or color graphs, charts and/or pictures, which have been reproduced in black and white.

- This document is paginated as submitted by the original source.

- Portions of this document are not fully legible due to the historical nature of some of the material. However, it is the best reproduction available from the original submission.

Produced by the NASA Center for Aerospace Information (CASI)

THEORY VERSUS EXPERIMENT FOR THE ROTORDYNAMIC[1]

COEFFICIENTS OF ANNULAR GAS SEALS:

PART 1, TEST FACILITY AND APPARATUS

Dara W. Childs, Professor

Clayton E. Nelson, Assistant Professor

Colby Nicks, Research Assistant[2]

Joseph Scharrer, Research Assistant

David Elrod, Research Assistant

Keith Hale, Research Engineer

Mechanical Engineering Department
Turbomachinery Laboratories
Texas A&M University
College Station, Texas   77843

Abstract

A facility and apparatus are described for determining the rotordynamic
coefficients and leakage characteristics of annular gas seals.   The
apparatus has a current top speed of 8000 cpm with a nominal seal
diameter of 15.24 cm (6 in).   The air-supply unit yields a seal
pressure ratio of approximately 7.   An external shaker is used to
excite the test rotor.   The capability to independently calculate all
rotordynamic coefficients   at   a given operating condition with one
excitation frequency.

INTRODUCTION

This paper describes the design, development, and operation of a test apparatus and facility which have been developed to measure leakage and rotordynamic coefficients for annular gas seals. By rotordynamic coefficients, we refer to the stiffness and damping coefficients which are used in the following linearized force-displacement model for seals

$$
-\begin{Bmatrix} F_X \\ F_Y \end{Bmatrix} = \begin{bmatrix} K_{XX} & K_{XY} \\ K_{YX} & K_{YY} \end{bmatrix} \begin{Bmatrix} X \\ Y \end{Bmatrix} + \begin{bmatrix} C_{XX} & C_{XY} \\ C_{YX} & C_{YY} \end{bmatrix} \begin{Bmatrix} \dot{X} \\ \dot{Y} \end{Bmatrix} \tag{1}
$$

where (X, Y) define the relative motion of the seal rotor relative to its stator, and (F_X F_Y) are the components of the reaction force acting on the rotor. Eq. (1) is assumed to apply for small motion about an arbitrary eccentricity position. For small motion about a centered position, the following simpler model applies

$$
-\begin{Bmatrix} F_X \\ F_Y \end{Bmatrix} = \begin{bmatrix} K & k \\ -k & K \end{bmatrix} \begin{Bmatrix} X \\ Y \end{Bmatrix} + \begin{bmatrix} C & c \\ -c & C \end{bmatrix} \begin{Bmatrix} \dot{X} \\ \dot{Y} \end{Bmatrix} \tag{2}
$$

As will be explained below, the test apparatus has the capability to separately identify the eight coefficients of Eq. (1) from measurements of seal motion and reaction forces.

Experience has shown that forces developed by plain annular gas seals may have a significant impact on the rotordynamic characteristics of turbines and compressors. This was demonstrated conclusively on the HPOTP (High Pressure Oxygen Turbopump) of the SSME (Space Shuttle Main Engine) where a change of the turbine interstage seal from a stepped-labyrinth, tooth-on-rotor configuration to a smooth-rotor,

honeycomb stator configuration eliminated serious synchronous and subsynchronous vibration problems [1]. Comparable stabilizing results have been achieved in commercial units by installing swirl webs upstream of labyrinth seals [2].

The test apparatus has been designed and used to measure rotordynamic coefficients of both plain annular seals (as used in floating-ring gas seals), plain seals with honeycomb stators, and labyrinth seals. Part 2 of this paper provides a comparison of test and theory for plain annular seals having constant-clearance and convergent-taper geometries. Subsequent publications will provide test results for honeycomb and labyrinth seals.

Prior Gas-Seal Test Approaches

The first systematic test program for measuring seal coefficients of annular gas seals was carried out by Wachter and Benchert at the Technical University of Stuttgurt [5]. Their apparatus yields only the direct (K) and cross-coupled (k) stiffness coefficients of Eq. (2). The seal rotor is statically displaced relative to its stator, the circumferential pressure distribution is measured and integrated, and the resultant reaction force is measured. Referring to Eq. (2), the static rotor displacement e_0 in the X direction yields

$$K = F_X/e_0, \qquad k = F_y/e_0$$

This approach obviously does not yield any damping values.

A second approach which has been used by Wright [6] uses a centered circular orbit defined by

$$X = e_0 \cos(\Omega t)$$

$$Y = e_0 \sin(\Omega t)$$

From Eq. (2) this yields the following radial and tangential coefficient definitions

$$Fr/\varepsilon_O = -c\Omega - K$$

$$F_\theta/\varepsilon_O = k - C\Omega$$

Wright used forward and backward orbits to define effective cross-coupled stiffness coefficients for single-cavity, turbine-tip seals.

External-Shaker Identification Approach

The parameter identification procedure of the present apparatus uses an external shaker procedure similar to that of Iino and Kaneko [8]. Figure 1 illustrated the conceptual approach to be used in calculating rotordynamic coefficients for small motion about the static eccentricity position defined by the coordinates (e_O, o). First harmonic horizontal motion is prescribed by defining

$$X = e_O + A \sin(\Omega t) + B \cos(\Omega t)$$

$$\dot{X} = A\Omega \cos(\Omega t) - B\Omega \sin(\Omega t)$$

$$Y = \dot{Y} = 0$$

This yields small motion parallel to the static eccentricity vector, where Ω is the shaking frequency. In a similar fashion, the X and Y-direction force components can be expressed

$$F_X = F_{XS} \sin(\Omega t) + F_{XC} \cos(\Omega t)$$

$$F_Y = F_{YS} \sin(\Omega t) + F_{YC} \cos(\Omega t)$$

(3)

Substituting these expressions into Eq. (2) and equating coefficients of sine and cosine terms yields the following four equations

$$F_{XS} = K_{XX} A - C_{XX} B$$

$$F_{XC} = K_{XX} B + C_{XX} A$$

$$F_{YS} = K_{YX} A - C_{YX} B \qquad (4)$$

$$F_{YC} = K_{YX} B + C_{YX} A$$

Solving this system of four equations in four unknowns defines the dynamic coefficients as

$$K_{XX}(\epsilon_0) = (F_{XC} B + F_{XS} A) / (A^2 + B^2)$$

$$K_{YX}(\epsilon_0) = (F_{YS} A + F_{YC} B) / (A^2 + B^2)$$

$$C_{XX}(\epsilon_0) = (F_{XC} A - F_{XS} B) / \Omega(A^2 + B^2) \qquad (5)$$

$$C_{YX}(\epsilon_0) = (F_{YC} A - F_{YS} B) / \Omega(A^2 + B^2)$$

Therefore, by measuring the transient reaction forces due to known rotor motion, determining the Fourier coefficients (A, B, F_{XS}, F_{XC}, F_{YS}, F_{YC}), and substituting into the above definitions, the indicated dynamic coefficients can be identified. If the rotor is shaken about a centered position, then the process is complete, since the linearized model of Eq. (2) has skew-symmetric stiffness and damping matrices. However, for the eccentric position illustrated the rotor must also be shaken vertically about the same position.

Defining vertical motion by

$$X = e_0, \qquad \dot{X} = 0$$

$$Y = A \sin(\Omega t) + B \cos(\Omega t) \qquad (6).$$

$$Y = A\Omega \cos(\Omega t) - B \cos(\Omega t),$$

and following the procedure outlined above for measurement and analysis of the reaction forces yields the following definitions for the remaining coefficients

$$K_{YY}(e_O) = (F_{XS} A + F_{XC} B) / (A^2 + B^2)$$

$$K_{XY}(e_O) = (F_{YC} B + F_{YS} A) / (A^2 + B^2)$$

$$C_{YY}(e_O) = (F_{XC} A - F_{XS} B) / \Omega(A^2 + B^2)$$

$$C_{XY}(e_O) = (F_{YS} B - F_{YC} A) / \Omega(A^2 + B^2)$$

(7)

Hence, for a given operating condition, all eight coefficients can be separately determined by alternately shaking the rotor in directions which are parallel and perpendicular to the static eccentricity vector. Only one excitation frequency Ω is required.

TEST HARDWARE

This section deals with the mechanical components and operation of the test apparatus, and provides answers to the following questions:

1) How is the static position of the seal rotor controlled?

2) How is the dynamic motion of the rotor executed and controlled?

3) How is compressed air obtained and supplied to the apparatus, and how is the pressure ratio across the seal controlled?

4) How is the incoming air prerotated before it inters the seal?

5) How are the seal rotor and stator mounted and replaced?

6) How is the seal rotor driven (rotated)?

Recalling the rotordynamic coefficient identification process described earlier, the external shaker method requires that the seal rotor be oscillated about a prescribed static position. The test apparatus meets those requirements by providing independent static and dynamic displacement control, which are described below.

Static Displacement Control. The test apparatus is designed to provide control over the static eccentricity position both horizontally and vertically within the seal. The rotor shaft is suspended in a pendulum- fashion from an upper, rigidly mounted pivot shaft, as shown in figures 2 and 3. This arrangement allows a side-to-side (horizontal) motion of the rotor, and a cam within the pivot shaft allows vertical positioning of the rotor.

The cam which controls the vertical position of the rotor is driven by a remotely-operated DC gearhead motor, allowing accurate positioning of the rotor during testing. Horizontal positioning of the

rotor is accomplished by a Zonic hydraulic shaker head and master controller, which provide independent static and dynamic displacement or force control. The shaker head is mounted on an I-beam supported structure, and can supply up to a 4450 N (1000 lbf) static force. The low frequency dynamic capability is also 4450N with an upper limit of 1000 Hz. As illustrated in figure 3, the shaker head output shaft acts on the rotor shaft bearing housing, and works against a return spring mounted on the opposite side of the bearing housing. The return spring maintains contact between the shaker head shaft and the bearing housing, thereby preventing hammering of the shaker shaft and the resulting loss of control over the horizontal motion of the rotor.

Dynamic Displacement Control. The dynamic motion of the seal rotor within the stator is horizontal. In addition to controlling the static horizontal position of the rotor, the Zonic shaker head moves the rotor through horizontal harmonic oscillations as the test is run. A Wavetek function generator provides the sinusoidal input signal to the Zonic controller, and both the amplitude and frequency of the rotor oscillations are controlled.

Although the test rig design provides for dynamic motion of the rotor in only the horizontal X-direction, all of the coefficients for either seal model (Eqs. (1) and (2)) can still be determined. As figure 4 shows, the required rotor motion perpendicular to the static eccentricity vector can be accomplished in an equivalent manner by statically displacing it the same amount (e_o) in the vertical direction and continuing to shake horizontally.

The test apparatus has a low first natural frequency of approximately 30 Hz, as illustrated by the Bode plots of figure 5. At frequencies above resonance, the force amplitudes required to achieve reasonable displacement amplitudes rises sharply. With the present apparatus, tests which have been performed at 27.2, 58.8, and 74.6 Hz and yield consistent results; however, tests at higher frequencies are not feasible.

In addition to providing control for the rotor's static position and dynamic motion, the test apparatus allows the following additional seal parameters to be controlled independently, providing insight into the influence these parameters have on seal behavior.

1) pressure ratio across the seal,

2) prerotation of the incoming fluid,

3) seal configuration, and

4) rotor rotational speed.

Pressure Ratio. The inlet air pressure and attendant mass flow rate through the seal are controlled by an electric-over-pneumatically actuated Masoneilan Camflex II, flow-control valve located upstream of the test section. An Ingersoll-Rand SSR-2000 single stage screw compressor rated at 34 m³/min @ 929 kPa (1200 scfm @ 120 psig) provides compressed air, which is then filtered and dried before entering a surge tank. Losses through the dryers, filters, and piping result in an actual maximum inlet pressure to the test section of approximately 772 kPa (90 psig) at a maximum flow rate of 27 m³/min (950 scfm). A four-inch inlet pipe from the surge tank supplies the test rig, and after passing through the seal, the air exhausts to atmosphere though a manifold with muffler.

Inlet Circumferential Velocity Control. In order to determine the effect of fluid rotation on the rotordynamic coefficients, the test rig design also allows for prerotation of the incoming air as it enters the seal. This prerotation introduces a circumferential component to the air flow direction, and is accomplished by guide vanes which direct and accelerate the flow towards the seal annulus. Inlet vanes are illustrated in figure 6. Three types of guide vanes are available; one rotates the flow in the direction of rotor rotation, another introduces no fluid rotation, and the third rotates the flow opposite the direction of rotor rotation. The two vane depths denoted by the dimension A in figure b are available.

Seal Configuration. The design of the test rig permits the installation of various rotor/stator combinations. As shown in figures 6 and 7, the stator is supported in the test section housing by three Kistler quartz load cells in a trihedral configuration. Figures 7 and 8 shown a smooth-rotor/smooth-stator seal, however, the apparatus can accept a variety of different seal designs. The seal rotor is press-fitted and secured axially by a bolt circle to the rotor shaft. Seals with different geometries (i.e., clearances, tapers, lengths) can be tested, as well as seals with different surface roughnesses. The replacement of these rotor/stator combinations can be accomplished with minimal downtime.

Rotational Speed. A Westinghouse 37.3 KW (50-hp) variable-speed electric motor drives the rotor shaft through a belt-driven jackshaft arrangement. This shaft is supported by two sets of Torrington hollow-roller bearings [8]. These bearings are extremely precise,

radially preloaded, and have a predictable and repeatable radial stiffness. Axial thrust due to the pressure differential across the seal is absorbed by a flat, roller-type, caged thrust bearing at the rear of the rotor. Both the shaft and thrust bearing at the rear of the rotor are lubricated by a positive-displacement gear-type oil pump.

Different jackshaft drive-pulleys can be fitted to provide up to a 4:1 speed increase from motor to rotor shaft, which would result in a rotor shaft speed range of 0-21,200 cpm. However, current design limitations, prevent the attainment of this upper rotational speed. High bearing temperatures, reduction of interference in the rotor-shaft fitment due to growth of the rotor with increasing speed, and excessive stresses in the drive-pulleys all serve to limit shaft speed. The highest rotational speed attained at the time of this writing is 8500 cpm, although modifications to allow higher speeds are in progress.

To conclude this discussion of the test hardware, two views of the complete test apparatus are included. Figure 9 shows the assembled rig, while an exploded view is provided in figure 10.

INSTRUMENTATION

Having discussed what seal parameters can he varied, and how the variations are implemented, separate measurement will now be discussed. The types of measurements which are made can be grouped into the following three categories:

1) rotor motion,

2) reaction-force measurements, and

3) fluid flow measurements.

These categories are described individually in the sections that follow.

Rotor-Motion Measurements. The position of the seal rotor within the stator is monitored by two Bently-Nevada eddy-current proximity probes, mounted in the test section housing. These probes are located 90 degrees apart, and correspond to the X and Y- directions. The proximity probes are used to determine the static position and dynamic motion of the rotor, and their resolution is 0.0025 mm (0.1 mil).

Reaction-Force Measurements. Reaction forces arise due to the static position and dynamic motion of the seal rotor within the stator. The reaction forces (F_X, F_y) exerted on the stator are measured by the three Kistler quartz load cells which support the stator in the test section housing. When the rotor is shaken, vibration is transmitted to the test section housing, both through the thrust bearing and through the housing mounts. The acceleration of the housing and stator generates unwanted inertial "ma" forces which are sensed by the load

cells, in addition to those pressure forces developed by the relative motion of the seal rotor and stator. For this reason, PCB piezoelectric accelerometers with integral amplifiers are mounted in the X and Y- directions on the stator, as shown in figure 8. These accels allow a (stator mass) x (stator acceleration) subtraction to the forces (F_X, F_Y) indicated by the load cells. With this correction, which is described more fully in the next section, only the pressure forces due to relative seal motion are measured.

Force measurement resolution is a function of the stator mass and the resolution of the load cells and accelerometers. Accelerometer resolution is 0.005 g, which must be multiplied by the stator mass in order to obtain an equivalent force resolution. The mass of the stator is 11.4 kg (25.2 lb); hence, force resolution for the accelerometers is 0.560 N (0.126 lb). Resolution of the load cells is 0.089 N (0.02 lb). Therefore, the resolution of the force measurement is limited by the accelerometers.

Fluid Flow Measurements. Fluid flow measurements include the leakage (mass flow rate) of air through the seal, the pressure gradient along the seal axis, the inlet fluid circumferential velocity, and the entrance pressure loss.

Leakage is measured with either a vortex flow- meter or a turbine flowmeter located in the piping upstream of the test section. Pressures and temperatures up and downstream of the meter are measured for mass flow rate determination. Resolution of the vortex and turbine

flowmeters are 0.0014 m³ (0.05 acf) and 1.47x10⁻⁵ m³ (5.18x10⁻⁴), respectively. The range of the vortex and turbine flowmeters are 37 to 534 and 3 to 60 acfm, respectively.

For measurement of the axial pressure gradient, the stator has pressure taps drilled along the length of the seal in the axial direction. These pressures, as well as all others, are measured with a 0-1.034 MPa (0-150 psig) Scanivalve differential-type pressure transducer through a 48 port, remotely-controlled Scanivalve model J scanner. Transducer resolution is 0.552 kPa (0.08 psi).

In order to determine the circumferential velocity of the air as it enters the seal, the static pressure at the guide vane exit is measured. This pressure, in conjunction with the measured flowrate and inlet air temperature, is used to calculate a guide vane exit Mach number. The compressible flow continuity equation

$$\dot{m} = P_{ex} A_{ex} M_{ex} [(\gamma/R_g T_t) (1 + (\gamma-1)M_{ex}^2 /2)]^{1/2} \qquad (7)$$

solved for M_{ex} where γ is the ratio of specific heats and R_g is the gas constant for air, T_t is the stagnation temperature of the air, p_{ex} is the static pressure at the vane exit, and A_{ex} is the total exit area of the guide vanes. Since all of the variables in the equation are either known or measured, the vane exit Mach number, and therefore the velocity, can be found.

In order to determine the circumferential component of this inlet velocity, a flow turning angle correction, in accordance with Cohen [21], is employed. The correction has been developed from guide vane cascade tests, and accounts for the fact that the fluid generally is not turned through the full angle provided by the shape of the guide vanes. With this flow deviation angle calculation, the actual flow

direction of the air leaving the vanes (and entering the seal) can be determined. Hence, the magnitude and direction of the inlet velocity is known, and the appropriate component is the measured inlet circumferential velocity.

DATA ACQUISITION AND REDUCTION

With the preceding explanations of how the seal parameters are varied, and how these parameters are measured, the discussion of how the raw data is processed and implemented can begin. Data acquisition is directed from a Hewlett-Packard 9816 (16-bit) computer with disk drive and 9.8 megabyte hard disk. The computer controls an H-P 6940B multiprogrammer which has 12-bit A/D and D/A converter boards and transfers control commands to and test data from the instrumentation.

As was previously stated, the major data groups are seal motion/reaction force data and fluid flow data. The motion/reaction force data are used for dynamic coefficient identification. The hardware involved includes the load cells, accelerometers, X-direction motion probe, a Sensotec analog filter unit, a tunable bandpass filter, and the A/D converter. The operation of these components is illustrated in figure 11, and their output is used in a serial sampling scheme which provides the computer with the desired data for reduction. Recalling the discussion of the reaction force measurements in the preceding section, a (stator mass) x (stator acceleration) subtraction from the indicated load cell forces is needed due to vibration of the stator and test section housing. This subtraction is performed with an analog circuit, and results in corrected F_X and F_Y force components due to relative seal motion.

The forced oscillatory shaking motion of the seal rotor is the key to the operation of the serial synchronous sampling (SSS) routine which is employed. The frequency of the rotor oscillation is set by a

function generator, and rotor motion is sensed by the X-direction motion probe. The motion signal is filtered by the narrow bandpass filter, and is used as a trigger signal for the SSS routine. Upon the operator's command, the SSS routine is enabled, and the next positive-to- negative crossing of the filtered motion signal triggers a quartz crystal clock/timer. Ten cycles of the corrected $F_X(t)$ signal are sampled, at a rate of 100 samples/cycle. The second positive-to-negative crossing of the filtered motion signal triggers the timer and initiates the sampling of ten cycles of the $F_X(t)$ signal. Finally, the third positive-to-negative crossing triggers the timer again, and ten cycles of the corrected $X(t)$ signal are sampled. Thus, at every test condition, 1000 data points are obtained for $F_X(t_i), F_Y(t_i)$, and $X(t_i)$, and the data arrays are stored in computer memory.

Some important points need to be stressed concerning this force/motion data acquisition. First, the bandpass filter is used only to provide a steady signal to trigger the timer/clock. Any modulation of the motion signal due to rotor motion at running speed is eliminated by this filter, provided the rotational frequency and shaking frequency are adequately separated. Therefore, the shaking frequencies are selected to avoid coincidence with running speeds. However, the rotor motion and corrected force signals which are sampled and captured for coefficient identification are filtered only by a low-pass filter (500 Hz cutoff), and the effects of runout as well as shaking motion are present in the recorded data. A second point worth noting is that the sample rate is directly dependent on the shaking frequency. As the shaking frequency is increased, the sample rate

(samples/second) also increases. In order to get the desired 100 samples/cycle, shaking frequencies must be chosen to correspond to discrete sample rates which are available. Hence, the frequency at which the rotor is shaken must be chosen to provide the desired sampling rate and a steady trigger signal.

Most of the fluid flow data are used as input parameters for seal analyses [3, 4, 10, 11]. The upstream (reservoir) pressure and temperature, downstream (sump) pressure, and the inlet circumferential velocity (determined as outlined earlier) are measured directly. Inlet losses and friction factors for seals must be obtained from axial-pressure gradient measurements.

TEST PROCEDURES

At the start of each test series, the force, pressure, and flowmeter systems are calibrated. The total system, from transducer to computer, is calibrated for each of these variables. The force system calibration utilizes a system of pulleys and known weights applied in the X and Y-directions. An air-operated dead-weight pressure tester is used for pressure system calibration, and flowmeter system calibration is achieved with an internal precision quartz clock which simulates a known flowrate.

All of the tests performed to date have been made with the rotor executing small motion about a centered position. A typical test begins by centering the seal rotor in the stator with the Zonic hydraulic shaker, starting airflow through the seal, setting the rotational speed of the rotor, and then beginning the shaking motion of the rotor. Data points are taken at rotational speeds of 200, 500, and 1000-8000 cpm, in 1000 cpm increments. At each rotational speed, the inlet pressure is varied and data points are taken over the pressure-range capacity of the system. For each test case (i.e., one particular running speed, shaking frequency, pressure ratio, and prerotation condition), the measured leakage, rotordynamic coefficients, axial pressure distribution, and entrance loss coefficient are determined and recorded.

This test sequence is followed for each shaking frequency, and for each inlet swirl condition. Therefore, fifty data points are taken per test (i.e. one shaking frequency and inlet swirl combination), with a total of nine tests (for small motion about a centered position) made per seal.

REFERENCES

1. Childs, D.W., and Moyer, D.S., "Vibration Characteristics of the HPOTP (High-Pressure Oxygen Turbopump) of the SSME ("Space Shuttle Main Engine)," ASME Paper No. 84-GT-31, 29th International Gas Turbine Conference and Exhibit, Amsterdam, 1984.

2. Ehric, F. and Childs, D., "Self-Excited Vibration in High-Performance Turbomachinery," Mechanical Engineering, Vol. 106/No. 5, May 1984, pp. 66-79.

3. Nelson, C.C., "Rotordynamic Coefficients for Compressible Flow in Tapered Annular Seals," Accepted for publication in the ASME Journal of Tribology.

4. Nelson, C.C., "Analysis for Leakage and Rotordynamic Coefficients of Surface-Roughened Tapered Annular Gas Seals," ASME Paper No. 84-GT-32, 1984. Texas A&M University.

5. Benckert, H., and Wachter, J., "Flow Induced Spring Coefficients of Labyrinth Seals for Application in Rotor Dynamics," NASA CP 2133, Rotordynamic Instability Problems in High-Performance Turbomachinery, proceedings of a workshop held at Texas A&M University, 12-14 May 1980.

6. Wright, D. V., "Air Model Test of Labyrinth Seal Forces on a Whirling Rotor," Report No. 77-1E7-SLVIB-P1, Westinghouse R&D Center, October 1972.

7. Iino, T., and Kaneko, H., "Hydraulic Forces Caused by Annular Pressure Seals in Centrifugal Pumps," NASA CP 2133, Rotordynamic Instability Problems in High-Performance Turbomachinery, proceedings of a workshop held at Texas A&M University, 12-14 May 1980.

8. Bowen, W. L., and Bhateje, R., "The Hollow Roller Rearing", ASME Paper No. 79-Lub-15, ASME-ASLE Lubrication Conference; Daton, Ohio, 16-18 October 1979.

9. Cohen, H., Rogers, G. F. C., and Scaravanamutto, H. I. H., Gas Turbine Theory, Longman Group Limited, 1972.

10. Childs, D., and Scharrer, J., "An Iwatsubo-Based Solution for Labyrinth Seals Comparison to Experimental Results", NASA CP 2338, Rotordynamic Instability Problems in High-Performance Turbomachinery, proceedings of a workshop held at Texas A&M University, 28-30 May 1984.

LIST OF FIGURES

Fig. 1 External shaker method used for coefficient identification.

PIVOT
SHAFT

RETURN
SPRING

ROTOR
HOUSING

SHAKER
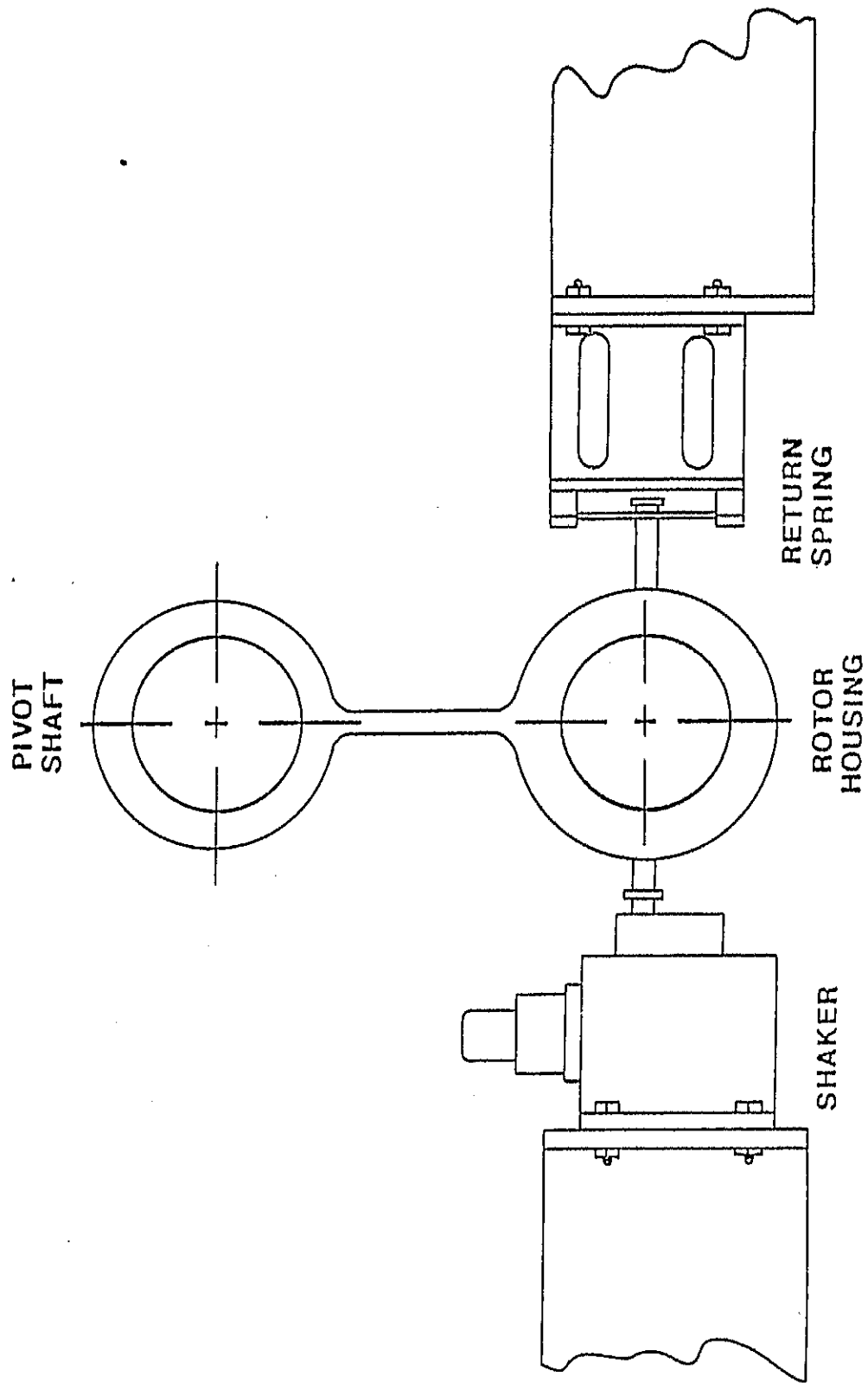
Fig. 2 Components used for static and dynamic displacement of seal rotor.

THRUST BEARING

LOAD CELL

PIVOT SHAFT

AIR IN

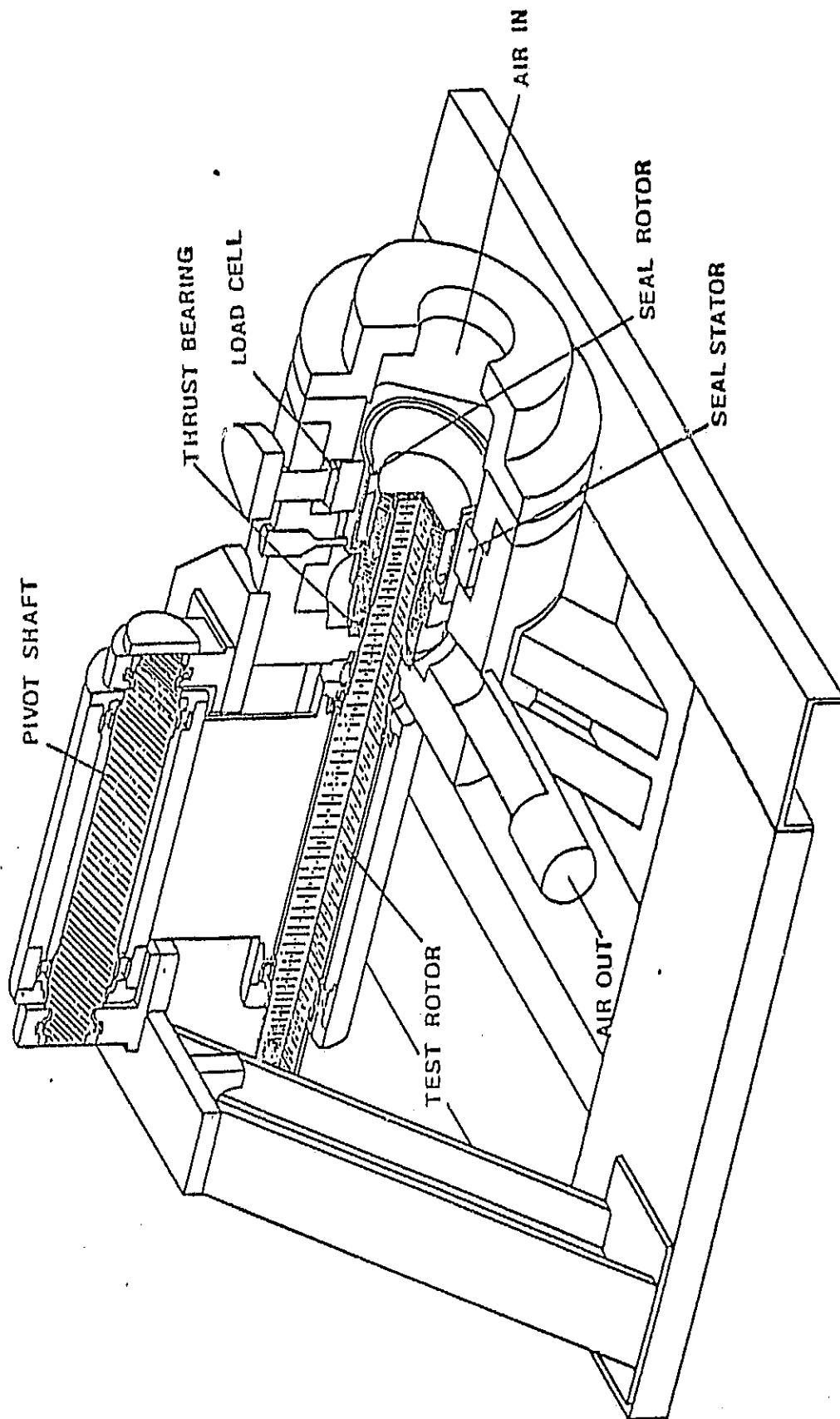SEAL ROTOR

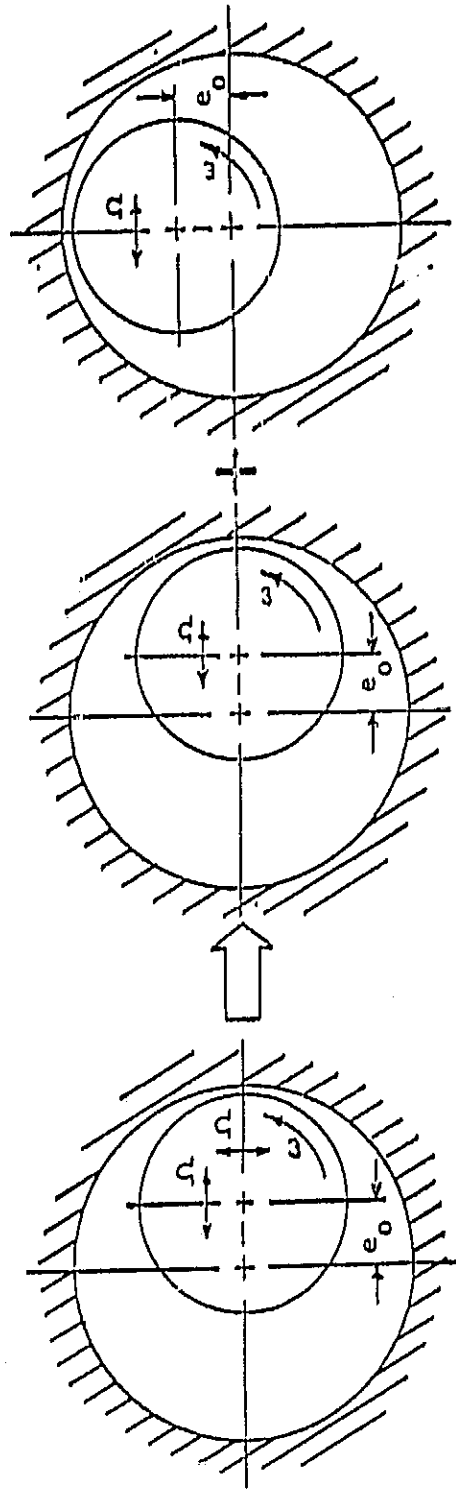SEAL STATOR

AIR OUT

TEST ROTOR

Fig. 3 Test apparatus.

Fig. 4   Shaking motion used for rotordynamic coefficient identification.
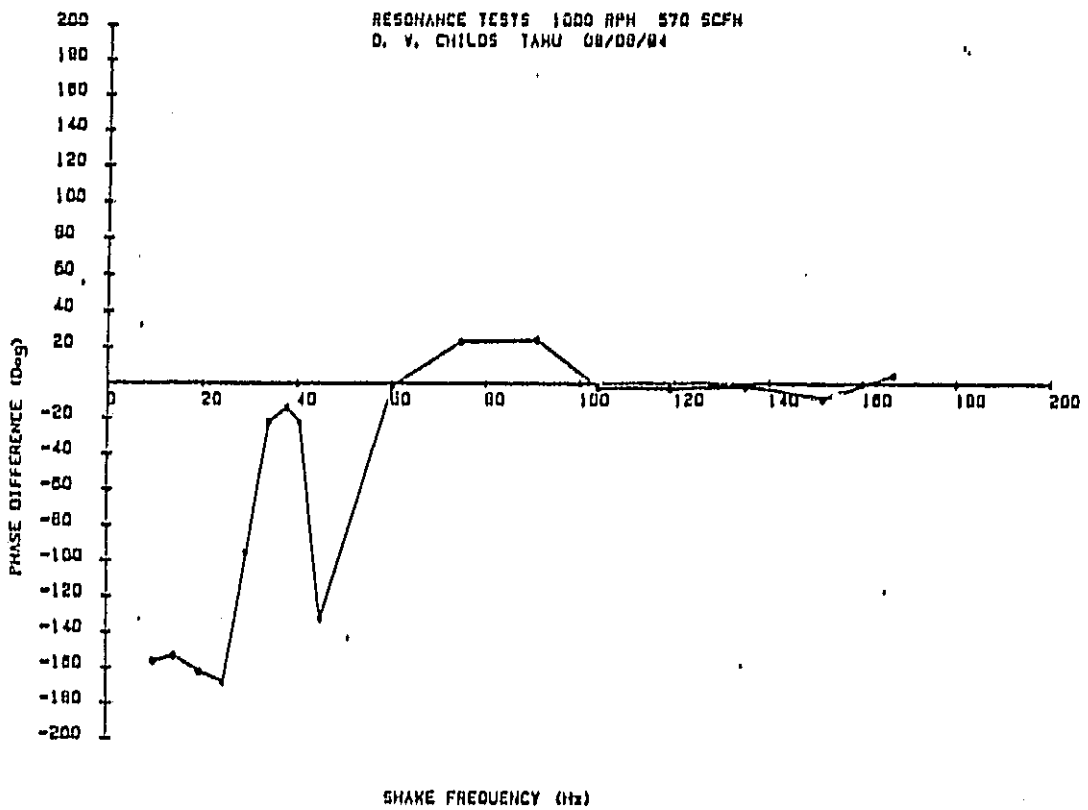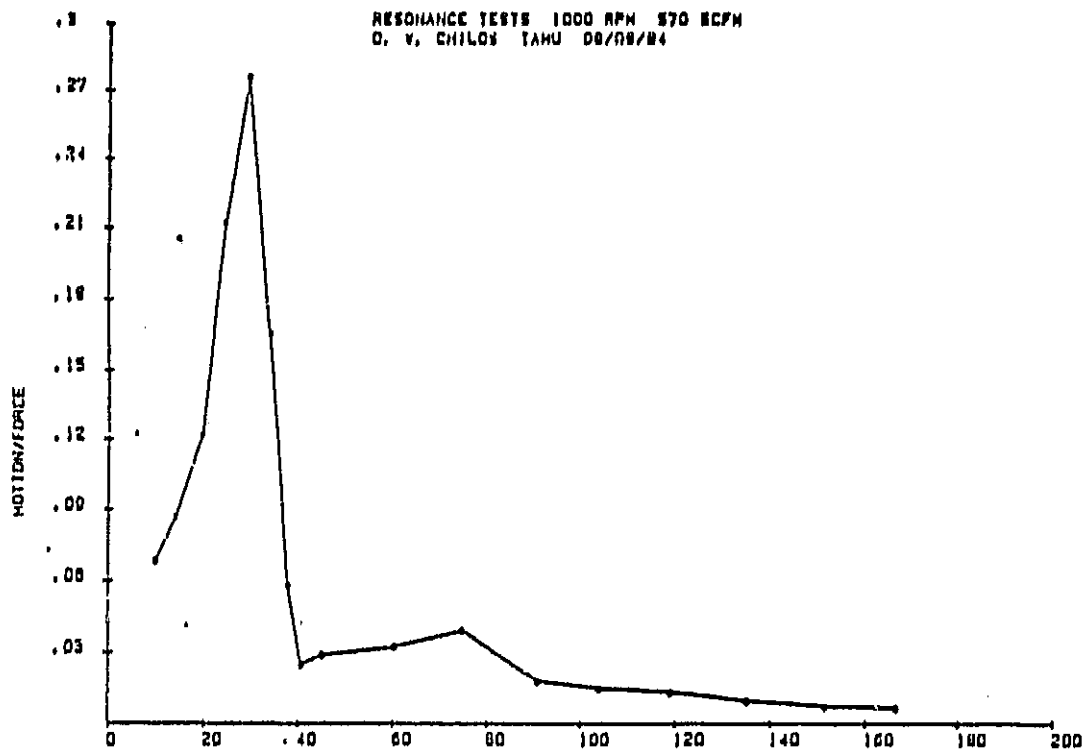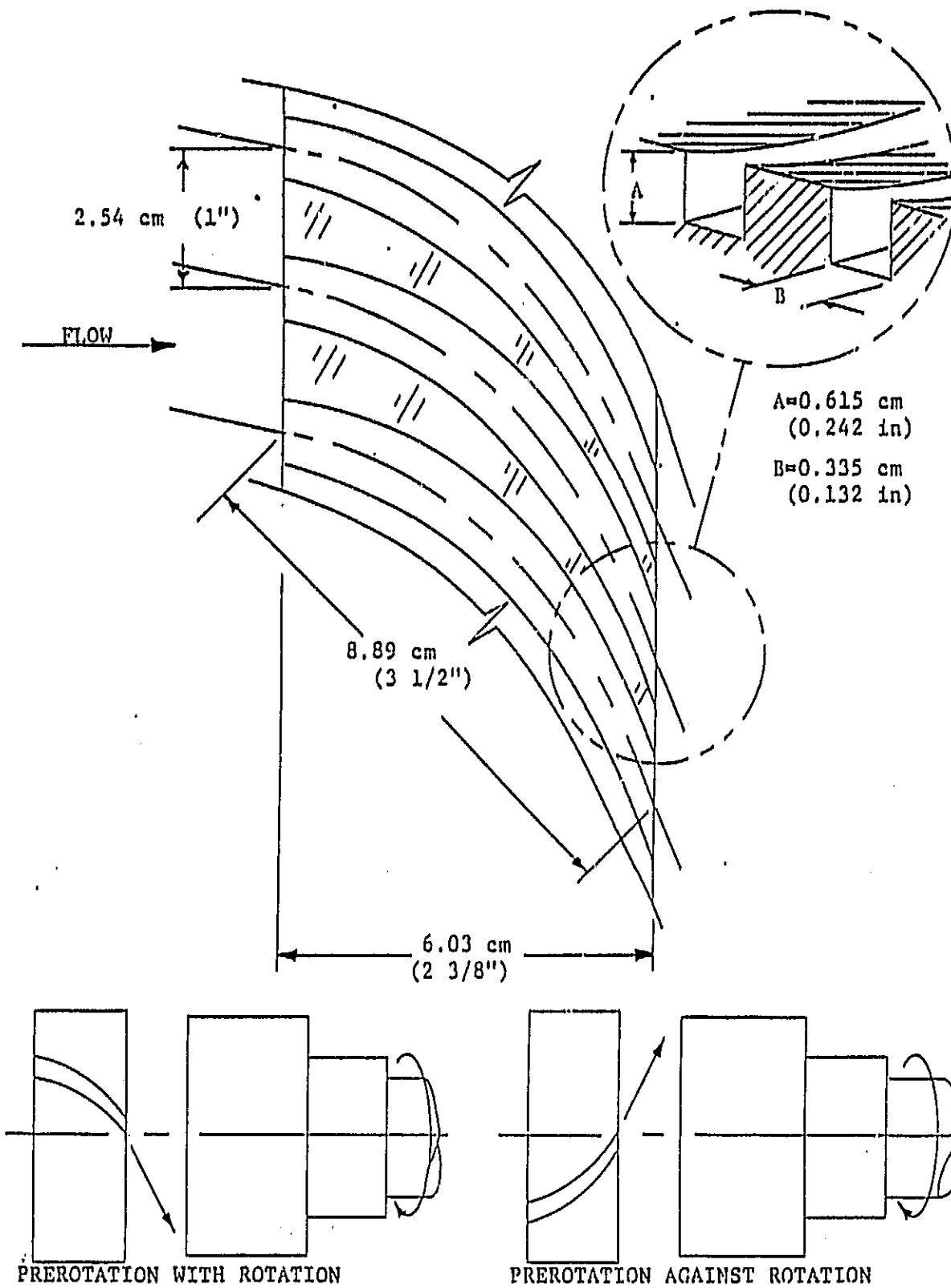
Fig. 5 Transfer function of test apparatus.

2.54 cm (1")

FLOW

A=0.615 cm
(0.242 in)

B=0.335 cm
(0.132 in)

8.89 cm
(3 1/2")

6.03 cm
(2 3/8")

PREROTATION WITH ROTATION   PREROTATION AGAINST ROTATION

Fig.6   Inlet guide vane detail.
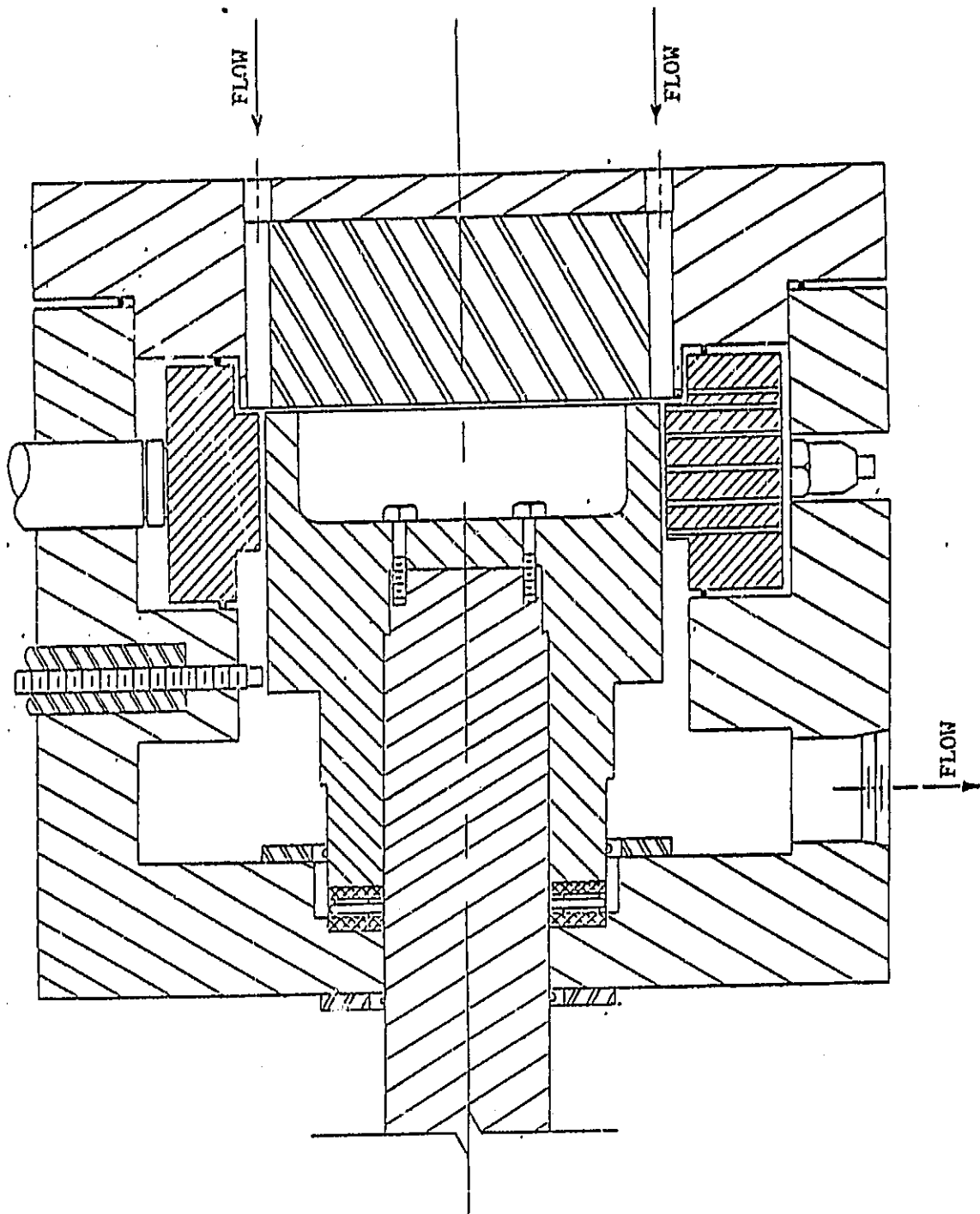
Fig. 7   Cross-sectional view of test section showing smooth stator.

PRESSURE
TAPS

LOAD CELLS (3)

FLOW

5,060 cm
(2.00")

15,283 cm
(6.017")

17.78 cm
(7")

ACCELEROMETERS (2)
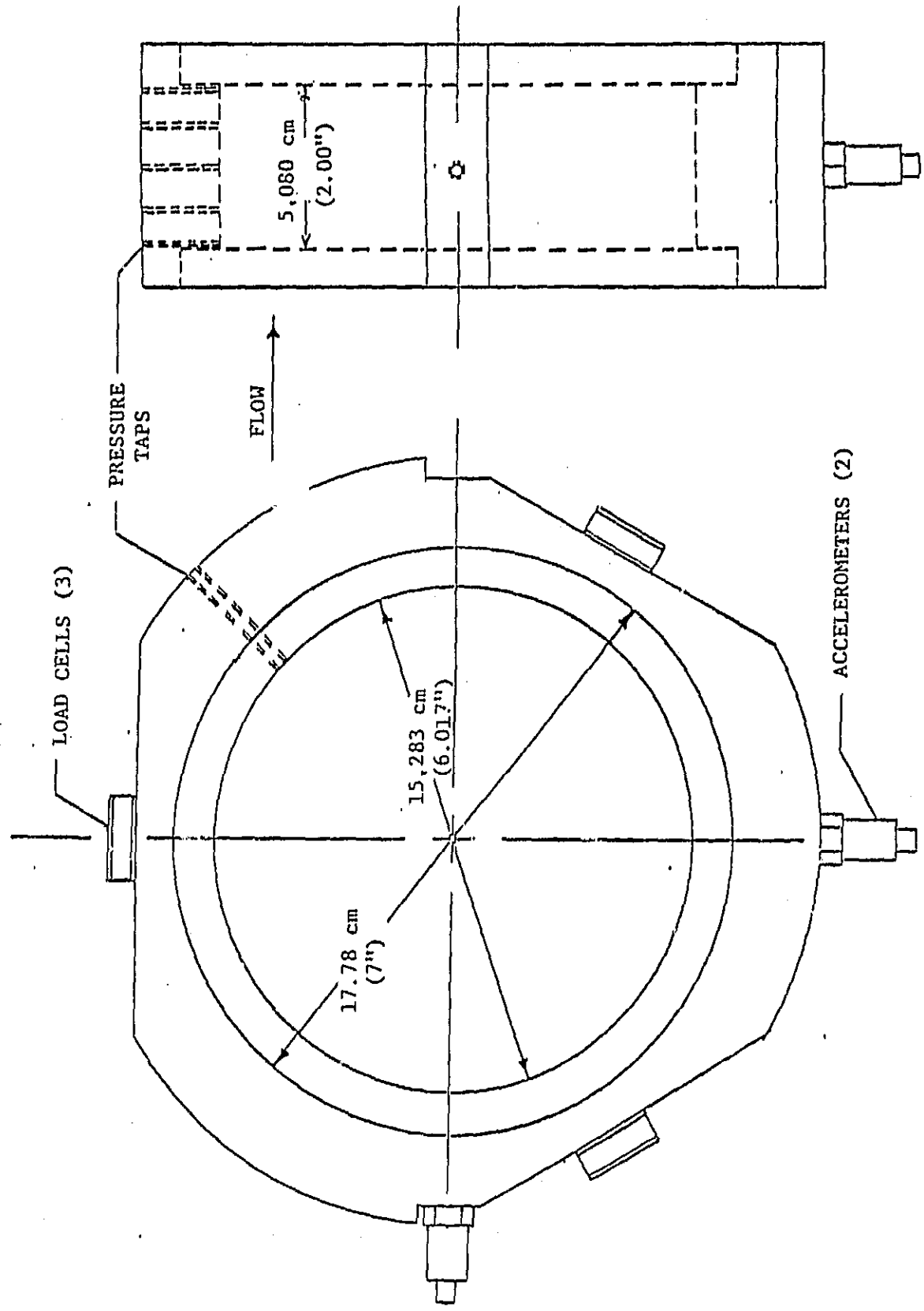
Fig. 8   Detail of smooth stator.

CONTROL VALVE

FLOWMETER

SHAKER SUPPORT STRUCTURE

TEST SECTION

SHAKER

DRIVE MOTOR
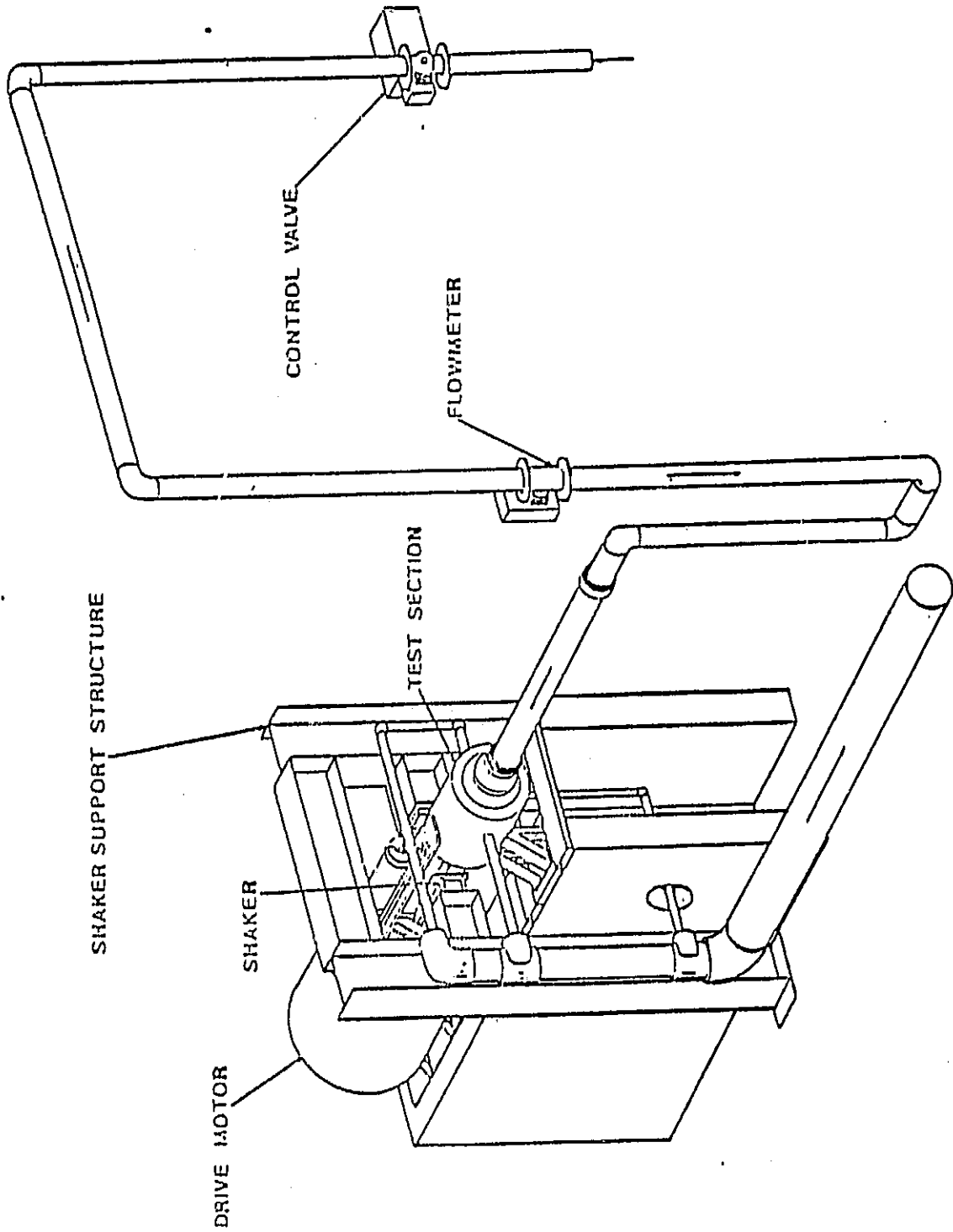
Fig. 9 Test apparatus assembly.

ELECTRIC MOTOR

JACKSHAFT & TOOTHED-DRIVE BELTS

PIVOT SHAFT

ROTOR SHAFT

TEST SECTION HOUSING

SEAL ROTOR

SEAL STATOR
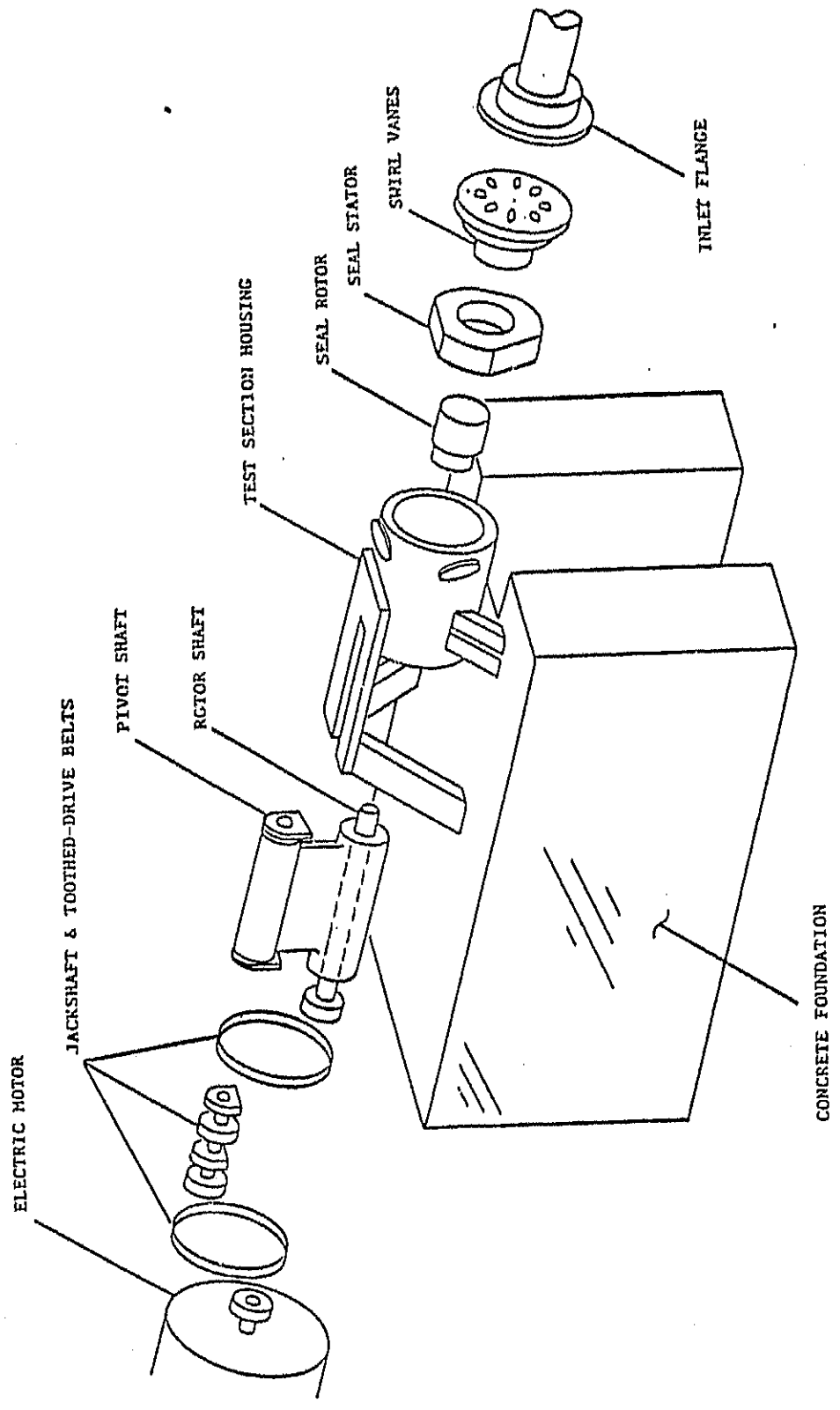
SWIRL VANES

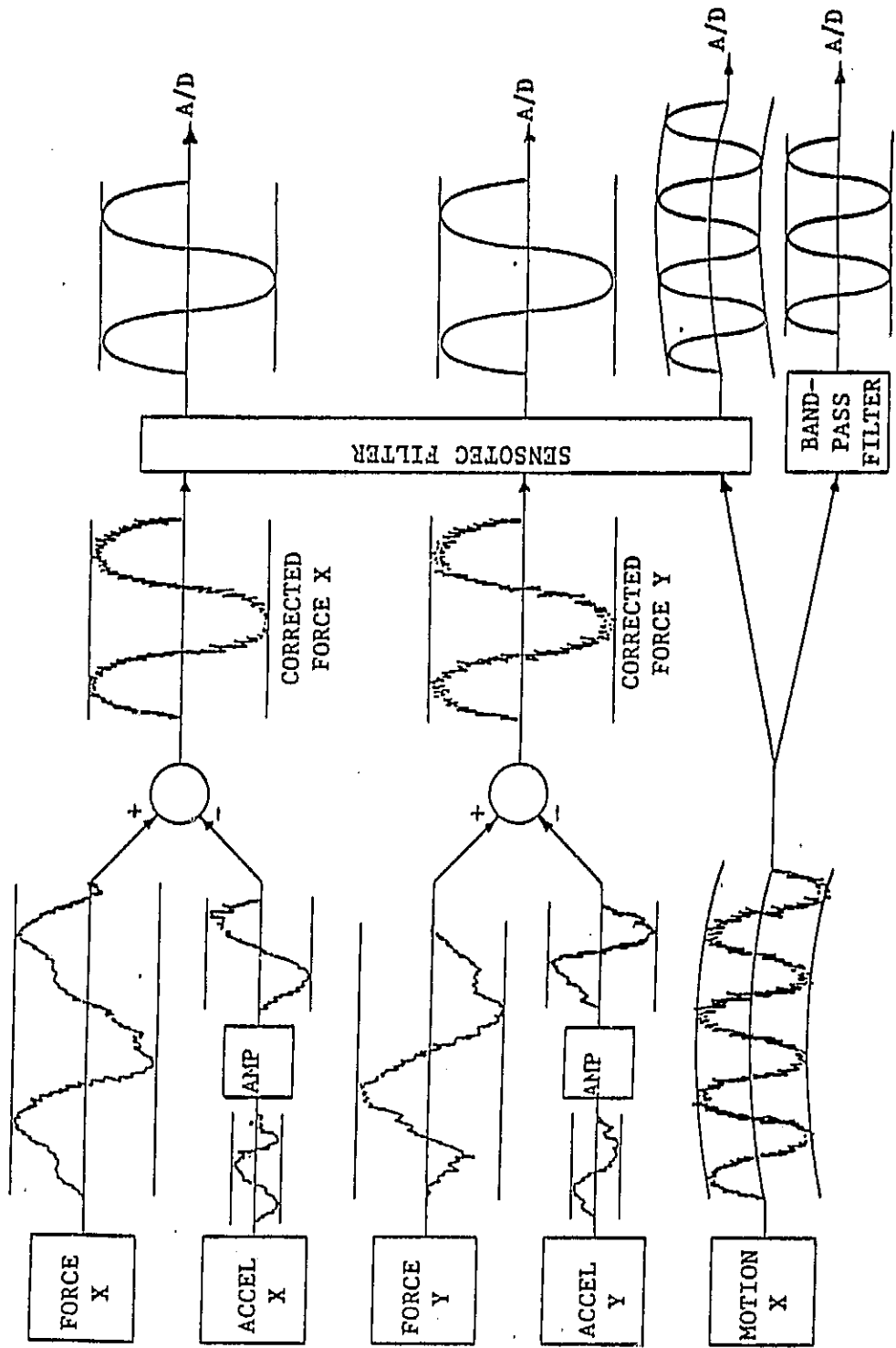INLET FLANGE

CONCRETE FOUNDATION

Fig. 10 Exploded view of test apparatus

Fig. 11 Signal conditioning schematic for data acquisition.